Myostatin propeptide-mediated amelioration of dystrophic pathophysiology

Sasha Bogdanovich,* Kelly J. Perkins,* Thomas O. B. Krag,*,† Lisa-Anne Whittemore,‡ and Tejvir S. Khurana*,[1]

*Department of Physiology and Pennsylvania Muscle Institute, University of Pennsylvania School of Medicine, Philadelphia, Pennsylvania, USA; †Department of Experimental Medicine, Glostrup Hospital, Glostrup, Denmark; and; ‡Cardiovascular and Metabolic Disease Department, Wyeth Research, Cambridge, Massachusetts, USA

ABSTRACT **Mutations in myostatin (GDF8) cause marked increases in muscle mass, suggesting that this transforming growth factor-β (TGF-β) superfamily member negatively regulates muscle growth. Myostatin blockade therefore offers a strategy for reversing muscle wasting in Duchenne's muscular dystrophy (DMD) without resorting to genetic manipulation. Here, we demonstrate that pharmacological blockade using a myostatin propeptide stabilized by fusion to IgG-Fc improved pathophysiology of the *mdx* mouse model of DMD. Functional benefits evidenced by specific force improvement, exceeded those reported previously using myostatin antibody-mediated blockade. More importantly, use of a propeptide blockade strategy obviates possibilities of anti-idiotypic responses that could potentially limit the effectiveness of antibody-mediated myostatin blockade strategies over time. This study provides a novel pharmacological strategy for treatment of diseases associated with muscle wasting such as DMD and since it uses an endogenous inhibitor of myostatin should help circumvent technical hurdles and toxicity associated with conventional gene or cell based therapies. *FASEB J.* 19, 543–549 (2005)**

Key Words: DMD · dystroglycan complex · neuromuscular disease · dystrophin · extracellular matrix

Duchenne's muscular dystrophy (DMD) is the most common X-linked neuromuscular disease and is estimated to affect 1 in 3500 newborn males. DMD is characterized by progressive and severe muscle loss that leads to loss of ambulation, with those affected often becoming wheelchair dependent toward the end of the first decade of life. The disease is caused by mutations in the *DMD* gene resulting in quantitative and/or qualitative disturbances in expression of the gene product, dystrophin (1, 2). Dystrophin is associated with the membrane-bound dystroglycan complex (DGC), which forms an important link with laminin, a constituent of the extracellular matrix. The DGC itself is part of a larger complex of evolutionary conserved proteins associated with dystrophin, including nNOS, dystroglycan, the sarcoglycans, syntrophins, dystrobrevin, and utrophin/DRP (3–5). Mutations in the genes encoding various members of the complex (and proteins binding members of the complex, e.g., α-2 laminin) are thought to disrupt sarcolemmal integrity, resulting in a variety of X-linked and limb girdle muscular dystrophies (LGMDs) (6). Mutations in genes not directly linked to the complex (e.g., emerin, dysferlin) can also result in certain types of muscular dystrophies (7–9). In the case of LGMD 2B, defective sarcolemmal repair due to dysferlin deficiency, rather than defective sarcolemmal integrity per se is thought to be mechanistic (10). Although DMD remains incurable, steady advances using gene-based, cell-based, and pharmacological strategies in experimental models of the disease continue to be made (11–13).

Myostatin (GDF8) is a member of the transforming growth factor-β (TGF-β) superfamily of growth/developmental factors. Myostatin is a negative regulator of muscle growth, with gene mutations leading to increased musculature in vivo. This is exemplified by the 20% increase in muscle mass seen in the naturally occurring "double-muscled" cattle first noted >200 years ago. Increased muscle mass due to myostatin mutations has been reported in mice (14–16), and more recently in humans (17). In common with other members of the TGF-β superfamily, myostatin consists of a ~26 kDa inactive N-terminal (also called the propeptide) region, an invariant tetrapeptide (RSRR) cleavage site, and an ~12 kDa active C-terminal (or mature) region. The gene and its modular organization have been extremely well conserved across evolution. The first 300 amino acids (encoding the inactive propeptide region) are 90% identical, whereas the tetrapeptide cleavage site in addition to the last 100 amino acids (encoding the active peptide) are 100% identical among human, mouse, chicken, and pig species. Analogous to other members of the TGF-β superfamily, the myostatin propeptide can bind and inhibit the activity of the active myostatin peptide in vitro.

[1] Correspondence: Department of Physiology and Pennsylvania Muscle Institute, A-601 Richards Building, University of Pennsylvania School of Medicine, 3700 Hamilton Walk, Philadelphia, PA 19104-6085, USA. E-mail: tsk@mail.med.upenn.edu

doi: 10.1096/fj.04-2796com

Furthermore, attenuation of myostatin activity using blocking antibodies, peptides, or pseudo-ligands has been demonstrated to increase muscle mass in mice in vivo (18–20).

We and others have hypothesized that increasing the myogenic/regenerative process by modulation of myostatin activity may improve the muscle weakness that is pathognomic of DMD (19, 21). Indeed, myostatin antibody-mediated blockade in vivo (19) was recently shown to functionally improve the phenotype of the *mdx* mouse model (22, 23) of DMD. In these experiments, 4-wk-old male *mdx* mice were treated for 3 months with weekly intraperitoneal (i.p.) injections of JA16 mouse monoclonal antibodies against myostatin at 60 mg/kg. The anatomical, biochemical, and physiological improvement achieved using blocking antibodies was considered promising since it circumvented technical hurdles and toxicity associated with conventional gene or cell-based therapies (19).

However, a complete reversal of phenotype was not achieved, as evidenced by lack of improvement in specific force. In an attempt to overcome these limitations as well as to extend previous studies, we describe the use of a novel propeptide-based myostatin inhibitor to investigate the effects of myostatin blockade on *mdx* mice in vivo.

MATERIALS AND METHODS

Injection of mice

Four-week-old male *mdx* mice were treated for 3 months with weekly i.p. injections of either recombinantly synthesized myostatin propeptide (14, 20, 24–26) fused with mouse Fc to improve stability in vivo (dose 10 mg/kg; treated *mdx* group) or equimolar amounts of mouse Fc alone (dose 5.7 mg/kg; control *mdx* group).

Physiological and biochemical studies

The myostatin propeptide fused to a murine IgG-Fc region (20, 24) and control mouse Fc peptide were obtained from Wyeth Research (Cambridge, MA, USA). The endogenous propeptide inhibits binding of myostatin to its receptor ActRIIB with an IC_{50} of 1 nM and the propeptide-Fc fusion inhibits myostatin with a similar affinity (24). Physiological properties of muscle were analyzed using freshly dissected ex vivo muscle from 16 wk-old-male *mdx* (C57BL/10ScSn-DMD$^{mdx/J}$) mice, as described previously (19, 27–29). Muscle length (Lo) was adjusted to achieve maximal twitch response. Eccentric contraction (ECC) force drop was calculated from the first and fifth tetanus of the standard ECC protocol, supramaximal stimulus of 700 ms (500 ms isometric phase, 200 ms eccentric phase), total lengthening Lo/10; lengthening velocity 0.5 Lo/s. At the end of physiological studies muscles were flash-frozen in liquid nitrogen cooled isopentane and stored at −80°C before sectioning. For biochemical assessment, serum was separated by centrifugation from tail vein blood that had previously been allowed to clot. Serum creatine kinase (CK) was measured using the indirect CK colorimetric assay kit and standards (Sigma, St. Louis, MO, USA).

Muscle morphology

Serial frozen sections (10 μm thickness) were cut at midbelly of muscle, subjected to gentle fixation using 100% ice cold methanol for 5 min, and stored in airtight containers at −80°C before analysis. Sections were processed for hematoxylin and eosin (H&E) staining for histology. For morphometric analysis sections were double labeled with anti-laminin monoclonal antibodies (Sigma) and the DNA binding dye Hoechst 33825, washed, incubated with Alexa 488-labeled goat anti-mouse antibodies, washed, mounted, and visualized using epi-fluorescence illumination on an Olympus BX 51 microscope. Pictures were taken using an Olympus Magnafire or Nikon Coolpix 950 Digital camera. Morphometric measurements were made on these digitized images using the Scion 4.02 image processing software (www.scioncorp.com). All myofibers (17,225) contained in the muscles physiologically evaluated in this study were imaged and scored for centrally nucleated fiber (CNF) determination. 5656 fibers were measured to calculate single fiber area.

Semiquantitative RT-PCR

For semiquantitative RT-PCR, total RNA isolation from *mdx* mouse tissue, subsequent cDNA synthesis and radiolabeled PCR analysis of utrophin and GAPDH were performed using primers and conditions as described previously (30).

Statistical analysis

ANOVA (**Fig. 1*a***) and Student's *t* test (all other figures) were used to determine statistical significance of results. The following convention is used for graphical representation:

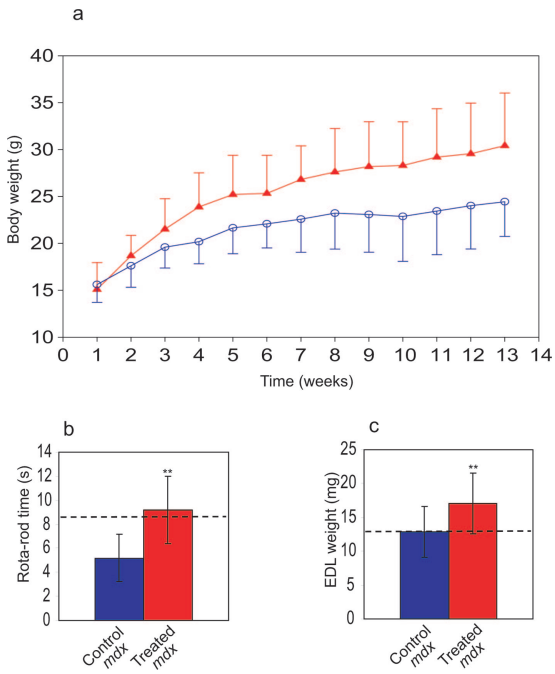

Figure 1. Consequences of propeptide-mediated myostatin blockade in *mdx* mice. Comparisons of growth curves (*a*), endurance time on a rota-rod (*b*) and EDL weight (*c*), between treated *mdx* mice (red) and control *mdx* mice (blue). Treated *mdx* mice had significantly different growth curves ($n=5$; ANOVA $P\leq0.001$), endurance time (9.2±2.8 vs. 5.2±1.9 s; $n=5$; *t* test $P<0.05$) and EDL weights (17.0±4.5 vs. 12.9±3.8 mg; $n=10$; *t* test $P<0.01$) compared with *mdx* controls.

mean ± SD; treated *mdx* mice, red; control *mdx* mice, blue; dashed line, data from age-matched C57BL/10 normal mice.

RESULTS

To determine overall consequences of propeptide-based myostatin blockade on *mdx* mice in vivo, we plotted growth curves of mice injected with the myostatin propeptide-Fc (treated group) or control Fc peptide (control group) after weighing the mice weekly. Figure 1*a* illustrates that growth was significantly accelerated in treated mice compared with controls. Previous studies have shown that *mdx* mice have diminished rota-rod performance (31). As demonstrated in Fig. 1*b*, the treated *mdx* mice had improved rota-rod performance, consistent with increased functional muscle and appropriately coordinated neuromuscular function in vivo. Increase in muscle mass was quantified by dissecting out and weighing individual *extensor digitorum longus* (EDL) muscles after sacrificing the animals. As shown in Fig. 1*c*, EDL muscles from the treated group of animals weighed significantly more than controls, consistent with previous observations on myostatin blockade (19, 25, 32).

To quantify physiological improvement of myostatin propeptide-treated muscle, we recorded maximum force produced upon field depolarization of freshly dissected EDL muscles ex vivo. **Figure 2*a–e*** illustrates a significant increase in maximal force produced during twitch and tetanic contraction in treated *mdx* mice. No significant differences were detected in twitch contraction time or half-relaxation time. Additional mechanical parameters are detailed in **Table 1**. Compared with antibody-mediated blockade (19), where tetanic force was increased proportional to increased muscle size (i.e., absolute force) but remained unchanged when normalized for increased size (i.e., specific force), propeptide-mediated blockade led to an increase in both absolute and specific tetanic force (Fig. 2*d, e*), demonstrating an improvement in an important index of disease pathophysiology.

Detailed morphometric analysis was performed to determine whether the increase in muscle mass and strength caused by propeptide-mediated myostatin blockade occurred due to hypertrophy or hyperplasia (see Table 1). As shown in **Fig. 3*a***, there was a significant increase in cross sectional area (CSA) of EDL from the treated group of mice. The average single fiber area was significantly increased compared with controls (Fig. 3*b*), suggesting true hypertrophy at the single myofiber level as evidenced by an overall shift of distribution. The average number of myofibers in the EDL remained relatively constant (Table 1), suggesting the increase in muscle mass was due to hypertrophy rather than hyperplasia. This is similar to results obtained with mice transgenically expressing a dominant negative myostatin propeptide molecule mutated at the cleavage site (16), as well as using blocking antibodies (19). A slight increase was noted in the number of CNF in the treated

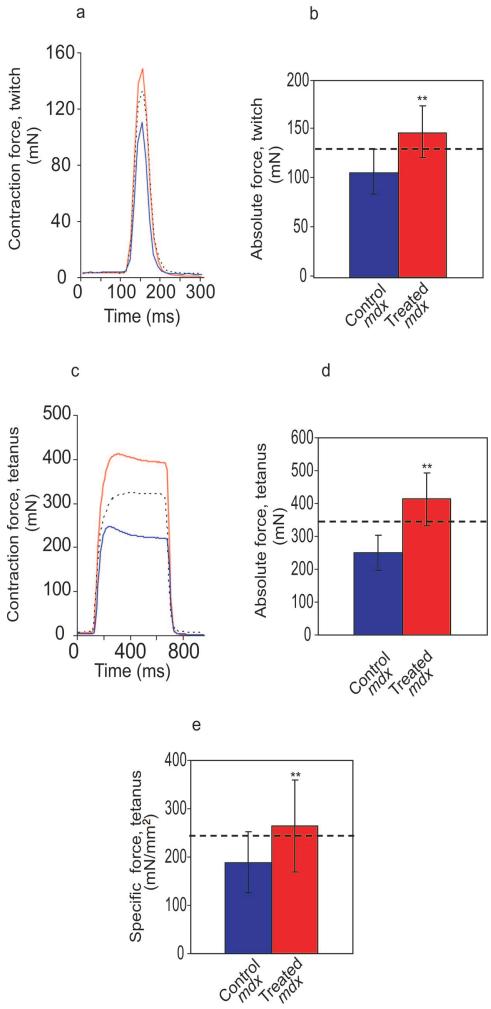

Figure 2. Increase of muscle strength by propeptide-mediated blockade in *mdx* mice. Comparisons of twitch (*a, b*) and tetanic force (*c–e*) between treated *mdx* mice (red) and control *mdx* mice (blue). Treated *mdx* mice generated greater absolute force during twitch *a)* representative traces; *b)* 146 ± 26.0 vs. 106 ± 22.3 mN; $n = 10$; *t* test $P < 0.0005$ and tetanic contraction; *c)* representative traces; *d)* 412.8 ± 81.3 vs. 250.6. ± 53.4 mN; $n = 10$; *t* test $P < 0.0007$. They generated greater specific force during tetanic contraction *e)* 263.9 ± 95.7 vs. 189.1 ± 62.4 mN/mm^2; n=10; *t* test $P \leq 0.01$.

group of *mdx* mice (Table 1), indicating fibers that had undergone prior regeneration (23). As CNFs are considered more resistant to necrosis, this finding suggests a potential mechanism by which myostatin blockade exerts beneficial effects in *mdx* mice (33). Indeed, increased regeneration is consistent with the predicted role of myostatin blockade enhancing proliferation of skeletal muscle precursors in vivo (34–36). Alternatively, increased myofiber stability may be a consequence of myostatin blockade enabling muscle growth above the level that can be compromised by normal workloads (37).

To determine whether propeptide-mediated myostatin blockade resulted in histological improvement, we performed additional analysis of muscle using H&E staining. Examination of EDL was equivocal; whereas evidence of prior degeneration and regeneration (in

TABLE 1. *Contractile and morphometric properties of EDL muscle*[a]

	Normal C57BL/10 ($n_{muscles}$=6)	Control *mdx* ($n_{muscles}$=10)	Treated *mdx* ($n_{muscles}$=10)
Twitch			
Absolute force (mN)	125.9 ± 39.6	106.1 ± 22.3	146.3 ± 26.0**
Specific force (mN/mm^2)	50.2 ± 30.9	37.5 ± 30.0	38.6 ± 20.4
Contraction time (ms)	63.3 ± 8.2	56 ± 13.5	53 ± 9.5
Half relaxation time (ms)	58.3 ± 14.7	53 ± 7.2	52 ± 9.4
Tetanus			
Absolute force (mN)	311.1 ± 103.1	250.6 ± 53.4	412.8 ± 81.3**
Specific force (mN/mm^2)	239.4 ± 110.4	189.1 ± 62.4	263.9 ± 95.7**
ECC force drop 1–5 (%)	42.7 ± 21.9	38.9 ± 27.7	33.2 ± 15.4
EDL weight (mg)	13.3 ± 3.2	12.9 ± 3.8	17.0 ± 4.5**
EDL Lo (mm)	13.2 ± 2.0	11.84 ± 0.7	13.3 ± 0.8**
CSA (mm^2)	1.5 ± 0.7	1.4 ± 0.5	1.8 ± 0.8**
CNF (%)	3.7 ± 1.1 (n_{fibres}=3656)	39.0 ± 9.1 (n_{fibres}=6551)	42.5 ± 5.9 (n_{fibres}=7081)
Single fiber area (μm^2)	1652.3 ± 865.2 (n_{fibres}=3656)	1317.1 ± 615.1 (n_{fibres}=1000)	1616.3 ± 674.9 (n_{fibres}=1000)**
Number of myofibers	609.0 ± 217.3	655.1 ± 139.9	708.1 ± 199.1

[a] Results are presented as mean ± SD; ** statistical significance ($P \leq 0.05$); CSA, cross sectional area; ECC, eccentric contraction; Lo, muscle length; CNF, centrally nucleated fibers.

the form of CNFs) was evident in both groups, insufficient foci of degeneration were observed to comment on improvement (unpublished data). We therefore examined the diaphragm, since this muscle group, in contrast to EDL, shows greater degenerative changes at 16 wk (38), the age at which this trial was terminated. A reduction in degenerative changes was observed in the diaphragm of treated *mdx* mice (**Fig. 4**), suggesting improvement of muscle pathology. We analyzed serum CK concentrations, since extremely high serum CK levels are noted in *mdx* mice and are considered a biochemical marker for sarcolemmal damage (39). At trial initiation, both groups of *mdx* mice had elevations of serum CK compared with normal mice. After 3 months of propeptide-mediated myostatin blockade, a decline in serum CK concentrations in treated *mdx* mice was noted (Fig. 4*c*), providing biochemical evidence for improvement due to myostatin propeptide-mediated blockade in vivo. To determine whether improvement was dependent on utrophin up-regulation, we analyzed utrophin mRNA expression levels in muscle; however, no difference was observed between treated and control *mdx* mouse muscle (**Fig. 5**). Improvement of the major functional indices, including increase in body weight, single fiber area, absolute and specific force generation, and reduction of serum CK, was noted in an independent pilot trial undertaken by us using 5 *mdx*-treated and 5 *mdx*-control mice (unpublished data).

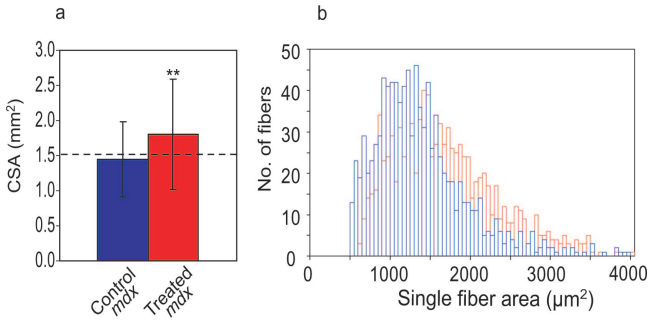

Figure 3. Increase of muscle size by propeptide-mediated blockade in *mdx* mice. Treated *mdx* mice (red bars) had larger CSA (*a*); 1.8 ± 0.5 vs. 1.4 ± 0.8 mm^2; $n = 10$; *t* test $P \leq 0.05$ and single fiber areas (*b*); 1616.3 ± 674.9 vs. 1317.1 ± 615.1 μm^2; $n_{fibers} = 2000$; *t* test $P < 0.0001$ compared with *mdx* controls (blue bars).

DISCUSSION

Correction of the muscle wasting pathognomic of DMD constitutes an important goal for a variety of therapeutic strategies (11–13, 40, 41). It is becoming increasingly apparent that this can be achieved not only by positive effectors of muscle growth (e.g., IGF-1) (42, 43), but also via repression of "negative" growth factors such as myostatin (GDF8) (19, 21), which inhibit muscle growth. We used the latter strategy in this study to demonstrate that myostatin blockade achieved by i.p. injections of a stabilized version of the myostatin propeptide resulted in a functional improvement of dystrophic pathophysiology in *mdx* mice. This strategy provides a novel pharmacological approach for treatment of diseases associated with muscle wasting and circumvents technical hurdles and toxicity associated with conventional gene or cell-based therapy. The use of this endogenously expressed molecule obviates the possibility of an anti-idiotypic response that could potentially limit effectiveness of antibody-mediated myostatin blockade strategy (19) over time. As sequence information for canine (K. J. Perkins and T. S. Khurana; AY367768) and human (19, 25) myostatin is available, species-specific propeptide molecule(s) can be readily generated for conducting preclinical

studies in the canine DMD model. If issues regarding the significantly higher costs, breeding difficulties, and phenotypic variability associated with the canine model can be satisfactorily circumvented by experimental design, preclinical testing of the myostatin propeptide approach in dystrophic dogs could facilitate efficient progression to clinical studies in patients, since the progressive muscle weakness and fibrosis observed for the canine DMD model more closely resembles human DMD than mice. In principle, synthesis of therapeutic propeptide molecules would overcome the potential delays and difficulties associated with identification and isolation of functional canine or humanized antibodies against myostatin for use in these species.

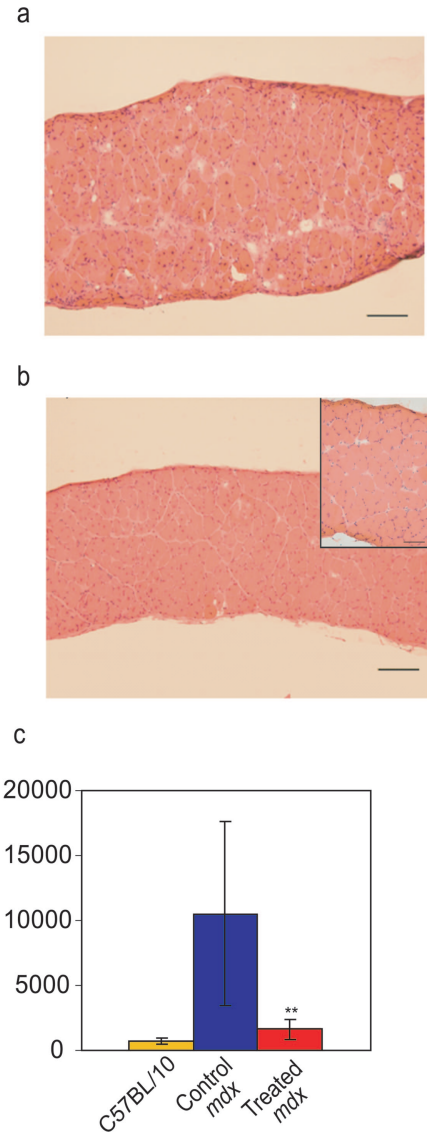

Figure 4. Reduction in muscle damage by propeptide-mediated myostatin blockade in *mdx* mice. Control *mdx* mice (*a*) had significantly greater pathological changes in the diaphragm compared with treated (*b*) *mdx* mice. Inset shows normal C57BL/10 mice. H&E staining; scale bar, 100 μm. *c)* Treated *mdx* mice (red) had significantly decreased serum CK concentrations compared with *mdx* controls (blue) (10491.7±7072.5 vs. 1611.7±723.6 U/l; $n=5$; t test $P \leq 0.05$). The levels were reduced significantly, but not to the low levels noted in normal age-matched C57BL/10 mice (yellow; 738.9±246.8 U/l; $n=9$).

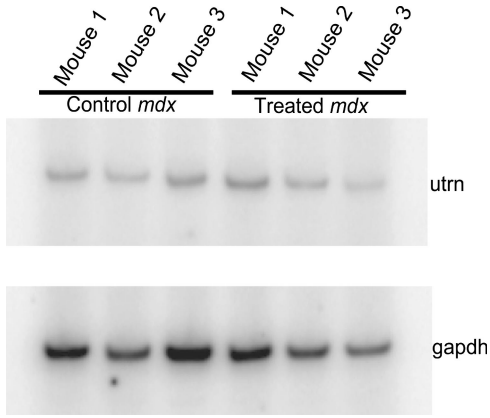

Figure 5. Propeptide-mediated myostatin blockade does not increase utrophin message levels. Treated *mdx* mice (top panel, right lanes) show no detectable increase of utrophin mRNA expression compared with control *mdx* mice (top panel, left lanes). Bottom panel shows GAPDH controls.

The degree of physiological improvement achieved using the propeptide approach exceeded the improvement achieved using murine antibody-mediated blockade (19), as evidenced by an improvement in specific force (**Table 2**). This may be related to the ~ 500-fold higher binding affinity of the propeptide moiety to myostatin compared with the blocking antibodies and/or the potential for the propeptide moiety to target GDF8 (myostatin) and closely related GDF11, rather than GDF8 alone. Improvement of specific force is a significant finding since it provides physiological evidence of a fundamental improvement in muscle mechanics using this pharmacological strategy. Though extremely encouraging, it is important to point out that no improvement was observed when using provocative ex vivo lengthening contraction protocols (Table 1), suggesting that the muscle remained susceptible to contraction-mediated damage (27, 28). This may be related to late onset and/or inadequate dosage of propeptide or a shared feature of strategies that seek to increase muscle mass in order to compensate for the dystrophic phenotype rather than directly replace the missing gene product (19, 37, 42, 43). These limitations could be overcome by combinatorial use with conventional gene/cell-based therapies or pharmacological approaches designed to correct specific functional deficits (44). The fact that such significant benefits were achieved independent of increased utrophin expression suggests that myostatin blockade could be further potentiated by combination with effectors of utrophin up-regulation known to

TABLE 2. *Comparison of antibody and propeptide-mediated myostatin blockade in mdx mice*

Parameter	Antibody treatment (% change) treated *mdx*/control *mdx* Bogdanovich et al. 2002	Propeptide treatment (% change) treated *mdx*/control *mdx* This study
Anatomical		
Body weight (g)	114%	124%
EDL weight (mg)	135%	132%
Index of EDL/Body weight	120%	108%
EDL Lo (mm)	106%	108%
EDL CSA (mm^2)	133%	129%
EDL single fiber area (μm^2)	125%	123%
Functional		
Absolute twitch force (mN)	134%	138%
Absolute tetanic force (mN)	132%	165%
Specific tetanic force (mN/mm^2)	102%	140%

improve ECC force drop (13, 29, 45). Experiments are currently under way to test these possibilities. FJ

T.S.K. was a paid consultant for Wyeth Research during the study. The study was supported in part by a grant from Wyeth Research to Glostrup Hospital (Denmark). S.B. was supported by a grant from the Muscular Dystrophy Association, USA. T.O.B.K. was supported by a predoctoral fellowship from the Faculty of Medicine, University of Copenhagen, Denmark.

REFERENCES:

1. Koenig, M., Hoffman, E. P., Bertelson, C. J., Monaco, A. P., Feener, C., and Kunkel, L. M. (1987) Complete cloning of the Duchenne muscular dystrophy (DMD) cDNA and preliminary genomic organization of the DMD gene in normal and affected individuals. *Cell* **50,** 509–517
2. Hoffman, E. P., Brown, R. H., Jr., and Kunkel, L. M. (1987) Dystrophin: the protein product of the Duchenne muscular dystrophy locus. *Cell* **51,** 919–928
3. Ervasti, J. M., and Campbell, K. P. (1991) Membrane organization of the dystrophin-glycoprotein complex. *Cell* **66,** 1121–1131
4. Matsumura, K., Ervasti, J. M., Ohlendieck, K., Kahl, S. D., and Campbell, K. P. (1992) Association of dystrophin-related protein with dystrophin-associated proteins in mdx mouse muscle. *Nature (London)* **360,** 588–591
5. Nishino, I., and Ozawa, E. (2002) Muscular dystrophies. *Curr. Opin. Neurol.* **15,** 539–544
6. Campbell, K. P. (1995) Three muscular dystrophies: loss of cytoskeleton-extracellular matrix linkage. *Cell* **80,** 675–679
7. Bione, S., Maestrini, E., Rivella, S., Mancini, M., Regis, S., Romeo, G., and Toniolo, D. (1994) Identification of a novel X-linked gene responsible for Emery-Dreifuss muscular dystrophy. *Nat. Genet.* **8,** 323–327
8. Bashir, R., Britton, S., Strachan, T., Keers, S., Vafiadaki, E., Lako, M., Richard, I., Marchand, S., Bourg, N., Argov, Z., et al. (1998) A gene related to *Caenorhabditis elegans* spermatogenesis factor fer-1 is mutated in limb-girdle muscular dystrophy type 2B. *Nat. Genet.* **20,** 37–42
9. Liu, J., Aoki, M., Illa, I., Wu, C., Fardeau, M., Angelini, C., Serrano, C., Urtizberea, J. A., Hentati, F., Hamida, M. B., et al. (1998) Dysferlin, a novel skeletal muscle gene, is mutated in Miyoshi myopathy and limb girdle muscular dystrophy. *Nat. Genet.* **20,** 31–36
10. Bansal, D., Miyake, K., Vogel, S. S., Groh, S., Chen, C. C., Williamson, R., McNeil, P. L., and Campbell, K. P. (2003) Defective membrane repair in dysferlin-deficient muscular dystrophy. *Nature (London)* **423,** 168–172
11. Kapsa, R., Kornberg, A. J., and Byrne, E. (2003) Novel therapies for Duchenne muscular dystrophy. *Lancet Neurol.* **2,** 299–310
12. Van Deutekom, J. C., and Van Ommen, G. J. (2003) Advances in Duchenne muscular dystrophy gene therapy. *Nat. Rev. Genet.* **4,** 774–783
13. Khurana, T. S., and Davies, K. E. (2003) Pharmacological strategies for muscular dystrophy. *Nat. Rev. Drug Discov.* **2,** 379–390
14. McPherron, A. C., Lawler, A. M., and Lee, S. J. (1997) Regulation of skeletal muscle mass in mice by a new TGF-beta superfamily member. *Nature (London)* **387,** 83–90
15. Szabo, G., Dallmann, G., Muller, G., Patthy, L., Soller, M., and Varga, L. (1998) A deletion in the myostatin gene causes the compact (Cmpt) hypermuscular mutation in mice. *Mamm. Genome* **9,** 671–672
16. Zhu, X., Hadhazy, M., Wehling, M., Tidball, J. G., and McNally, E. M. (2000) Dominant negative myostatin produces hypertrophy without hyperplasia in muscle. *FEBS Lett.* **474,** 71–75
17. Schuelke, M., Wagner, K. R., Stolz, L. E., Hubner, C., Riebel, T., Komen, W., Braun, T., Tobin, J. F., and Lee, S. J. (2004) Myostatin mutation associated with gross muscle hypertrophy in a child. *N. Engl. J. Med.* **350,** 2682–2688
18. Lee, S. J., and McPherron, A. C. (2001) Regulation of myostatin activity and muscle growth. *Proc. Natl. Acad. Sci. USA* **98,** 9306–9311
19. Bogdanovich, S., Krag, T. O., Barton, E. R., Morris, L. D., Whittemore, L. A., Ahima, R. S., and Khurana, T. S. (2002) Functional improvement of dystrophic muscle by myostatin blockade. *Nature (London)* **420,** 418–421
20. Wolfman, N. M., McPherron, A. C., Pappano, W. N., Davies, M. V., Song, K., Tomkinson, K. N., Wright, J. F., Zhao, L., Sebald, S. M., Greenspan, D. S., et al. (2003) Activation of latent myostatin by the BMP-1/tolloid family of metalloproteinases. *Proc. Natl. Acad. Sci. USA* **100,** 15842–15846
21. Wagner, K. R., McPherron, A. C., Winik, N., and Lee, S. J. (2002) Loss of myostatin attenuates severity of muscular dystrophy in mdx mice. *Ann. Neurol.* **52,** 832–836
22. Hoffman, E. P., Monaco, A. P., Feener, C. C., and Kunkel, L. M. (1987) Conservation of the Duchenne muscular dystrophy gene in mice and humans. *Science* **238,** 347–350
23. Coulton, G. R., Curtin, N. A., Morgan, J. E., and Partridge, T. A. (1988) The mdx mouse skeletal muscle myopathy: II. Contractile properties. *Neuropathol. Appl. Neurobiol.* **14,** 299–314
24. Thies, R. S., Chen, T., Davies, M. V., Tomkinson, K. N., Pearson, A. A., Shakey, Q. A., and Wolfman, N. M. (2001) GDF-8 propeptide binds to GDF-8 and antagonizes biological activity by inhibiting GDF-8 receptor binding. *Growth Factors* **18,** 251–259
25. McPherron, A. C., and Lee, S. J. (1997) Double muscling in cattle due to mutations in the myostatin gene. *Proc. Natl. Acad. Sci. USA* **94,** 12457–12461
26. Hill, J. J., Davies, M. V., Pearson, A. A., Wang, J. H., Hewick, R. M., Wolfman, N. M., and Qiu, Y. (2002) The myostatin

propeptide and the follistatin-related gene are inhibitory binding proteins of myostatin in normal serum. *J. Biol. Chem.* **277,** 40735–40741
27. Petrof, B. J., Shrager, J. B., Stedman, H. H., Kelly, A. M., and Sweeney, H. L. (1993) Dystrophin protects the sarcolemma from stresses developed during muscle contraction. *Proc. Natl. Acad. Sci. USA* **90,** 3710–3714
28. Moens, P., Baatsen, P. H., and Marechal, G. (1993) Increased susceptibility of EDL muscles from mdx mice to damage induced by contractions with stretch. *J. Muscle Res. Cell Motil.* **14,** 446–451
29. Krag, T. O., Bogdanovich, S., Jensen, C. J., Fischer, M. D., Hansen-Schwartz, J., Javazon, E. H., Flake, A. W., Edvinsson, L., and Khurana, T. S. (2004) Heregulin ameliorates the dystrophic phenotype in mdx mice. *Proc. Natl. Acad. Sci. USA* **101,** 13856–13860
30. Khurana, T. S., Rosmarin, A. G., Shang, J., Krag, T. O., Das, S., and Gammeltoft, S. (1999) Activation of utrophin promoter by heregulin via the ets-related transcription factor complex GA-binding protein alpha/beta. *Mol. Biol. Cell* **10,** 2075–2086
31. Muntoni, F., Mateddu, A., Marchei, F., Clerk, A., and Serra, G. (1993) Muscular weakness in the mdx mouse. *J. Neurol. Sci.* **120,** 71–77
32. Whittemore, L. A., Song, K., Li, X., Aghajanian, J., Davies, M., Girgenrath, S., Hill, J. J., Jalenak, M., Kelley, P., Knight, A., et al. (2003) Inhibition of myostatin in adult mice increases skeletal muscle mass and strength. *Biochem. Biophys. Res. Commun.* **300,** 965–971
33. Matsuda, R., Nishikawa, A., and Tanaka, H. (1995) Visualization of dystrophic muscle fibers in mdx mouse by vital staining with Evans blue: evidence of apoptosis in dystrophin-deficient muscle. *J. Biochem. (Tokyo)* **118,** 959–964
34. McCroskery, S., Thomas, M., Maxwell, L., Sharma, M., and Kambadur, R. (2003) Myostatin negatively regulates satellite cell activation and self-renewal. *J. Cell Biol.* **162,** 1135–1147
35. Amthor, H., Huang, R., McKinnell, I., Christ, B., Kambadur, R., Sharma, M., and Patel, K. (2002) The regulation and action of myostatin as a negative regulator of muscle development during avian embryogenesis. *Dev. Biol.* **251,** 241–257
36. Langley, B., Thomas, M., Bishop, A., Sharma, M., Gilmour, S., and Kambadur, R. (2002) Myostatin inhibits myoblast differentiation by down-regulating MyoD expression. *J. Biol. Chem.* **277,** 49831–49840
37. Zammit, P. S., and Partridge, T. A. (2002) Sizing up muscular dystrophy. *Nat. Med.* **8,** 1355–1356
38. Stedman, H. H., Sweeney, H. L., Shrager, J. B., Maguire, H. C., Panettieri, R. A., Petrof, B., Narusawa, M., Leferovich, J. M., Sladky, J. T., and Kelly, A. M. (1991) The mdx mouse diaphragm reproduces the degenerative changes of Duchenne muscular dystrophy. *Nature (London)* **352,** 536–539
39. Bulfield, G., Siller, W. G., Wight, P. A., and Moore, K. J. (1984) X chromosome-linked muscular dystrophy (mdx) in the mouse. *Proc. Natl. Acad. Sci. USA* **81,** 1189–1192
40. Bogdanovich, S., Perkins, K. J., Krag, T. O., and Khurana, T. S. (2004) Therapeutics for Duchenne muscular dystrophy: current approaches and future directions. *J. Mol. Med.* **82,** 102–115
41. Sohn, R. L., and Gussoni, E. (2004) Stem cell therapy for muscular dystrophy. *Expert Opin. Biol. Ther.* **4,** 1–9
42. Lynch, G. S., Cuffe, S. A., Plant, D. R., and Gregorevic, P. (2001) IGF-I treatment improves the functional properties of fast- and slow-twitch skeletal muscles from dystrophic mice. *Neuromuscul. Disord.* **11,** 260–268
43. Barton, E. R., Morris, L., Musaro, A., Rosenthal, N., and Sweeney, H. L. (2002) Muscle-specific expression of insulin-like growth factor I counters muscle decline in mdx mice. *J. Cell Biol.* **157,** 137–148
44. Bachrach, E., Li, S., Perez, A. L., Schienda, J., Liadaki, K., Volinski, J., Flint, A., Chamberlain, J., and Kunkel, L. M. (2004) Systemic delivery of human microdystrophin to regenerating mouse dystrophic muscle by muscle progenitor cells. *Proc. Natl. Acad. Sci. USA* **101,** 3581–3586
45. Tinsley, J., Deconinck, N., Fisher, R., Kahn, D., Phelps, S., Gillis, J. M., and Davies, K. (1998) Expression of full-length utrophin prevents muscular dystrophy in mdx mice. *Nat. Med.* **4,** 1441–1444

Received for publication September 14, 2004.
Accepted for publication December 2, 2004.